ICAS-88-2.6.2

DETAILED MEASUREMENTS OF THE FLOW IN THE VANED DIFFUSER OF A BACKSWEPT TRANSONIC CENTRIFUGAL IMPELLER

by

Ch. FRADIN

Office National d'Etudes et de Recherches Aérospatiales
BP 72 - 92322 Châtillon Cedex, France

16ème Congrès ICAS, JERUSALEM (1988)

Abstract

Detailed measurements have been made of the flow field in the vaned diffuser of a centrifugal compressor using miniature pressure probes and hot wire anemometers.

The rotor used in a backswept transonic centrifugal impeller with mid-channel splitter vanes. The tests are performed in a freon loop at the design mass flow rate of the compressor.

To understand how the flow field is structured and how it varies with time, detailed investigations are undertaken in the throat and at the outlet of the vaned diffuser.

Contour maps of the time-averaged flow angles and Mach numbers show the strong heterogeneities of the flow field in the tested sections.

Time-dependent measurements performed in the vaned diffuser throat show the large variations of the instantaneous flow angles and Mach numbers as a function of the impeller blade location. In the middle of the throat, unsteady flow angle deviations of eight degrees occur and the Mach number flow fluctuations reach 12 %.

At the diffuser channel outlet, more flow vanishes in the vicinity of the suction side and separation appears near the pressure side.

The performance of each parts of the vaned diffuser can be determined using mean values of the flow parameters.

Nomenclature

A	Local area
a	Velocity of sound
B	Blockage ratio
C_p	Static pressure recovery
K	Loss coefficient
M	Mach number
P	Pressure
Q	Mass flow
r	Gas constant
S	Entropy
t, T	Time, period
T	Temperature
α	Absolute angle
γ	Isentropic exponent
η	Efficiency
π	Pressure ratio
ρ	Fluid density
ζ	Dimensionless depth

Subscript

1	Inlet compressor condition
i	Total condition
-	Averaged property

Introduction

The flow field in the high-performance transonic compressor is difficult to investigate analytically, due to the three-dimensional curvature of the streamlines, the shock waves, the viscosity and the secondary flows.

Particular difficulty exists at the exit of the impeller, in the vaneless diffuser and in the semi-vaneless diffuser. It is well-known that the flow from the impeller is highly distorted [1] [2] with axial heterogeneities and large unsteady tangential heterogeneities due to the blades and splitter vanes of the rotor. There are also large steady tangential distortions generated by the interactions of the diffuser blades on the flow streamlines.

So the prediction of the behaviour of an unsteady heterogeneous flow field in the semi-vaneless diffuser and in the diffuser is currently unsatisfactory and analytical methods are still being developed.

For this purpose, experimental investigations are needed to define satisfactory boundary conditions and validate the computation results.

The flow field structure at the vaned diffuser outlet is also of use in optimizing the next stage of the compressor.

To obtain such results, tests have been run on vaned diffuser at nominal mass flow and nominal rotation speed.

The rotor is of the backward leaning blades type with mid-channel splitter vanes. The vaned diffuser in use is of the camber vane type.

Test facility

The impeller and the vaned diffuser tested are shown in Fig. 1. Their main characteristics are given in Tables I and II.

The splitter vanes are located at mid-channel and their geometries are identical to those of the main blades.

The impeller in use for this study has been tested in numerous investigations.

Initially, it was equipped with a large vaneless diffuser, in order to get more details on the flow field in the impeller outlet. Detailed flow measurements performed in the vaneless diffuser show that the blade-to-blade flow heterogeneities decay slowly in it. However, the transverse heterogeneities become even larger going downstream and flow separations may even occur [3].

Figure 2 gives a schematic representation of the test facility. The hub in front of the impeller provides a converging channel which simulates the effect of upstream axial flow compressors. Uniform total pressure and swirl-free flow are obtained at the rotor inlet.

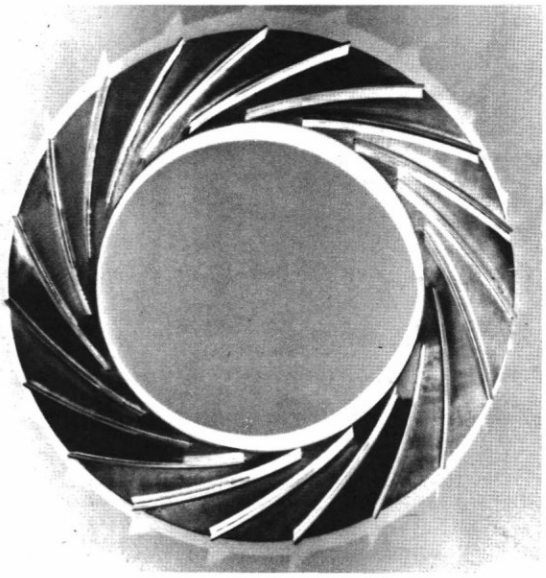

Fig. 1 — The impeller and the vaned diffuser.

Inlet	
- Hub diameter (mm)	100
- Tip diameter (mm)	173
- Number of blades	13
- Angle of the blades from axial direction (tip diameter)	62.54°
- Absolute Mach number	0.324
Outlet	
- Diameter (mm)	294
- Width of the channel (mm)	11
- Number of blades	26
- Angle of the blades from radial direction	30°
- Peripheral Mach number	1.189
Rotating speed (rpm)	9660

Table I : Impeller design parameters.

- Vane number	19
- Diffuser depth (mm)	11
- Throat aspect ratio	1.527
- Exit diffuser channel aspect ratio	3.394
- Ratio of diffuser leading edge radius to impeller exit radius	1.034
- Ratio of diffuser trailing edge radius to impeller exit radius	1.527
- Vane leading edge angle	15.3°
- Vane trailing edge angle	36.7°
- Diffuser channel divergence angle	$2\alpha = 8°$

Table II : Diffuser design parameters.

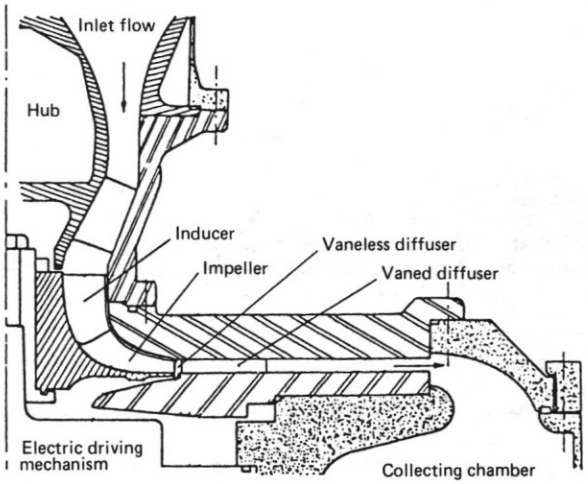

Fig. 2 — Compressor test rig schema.

A closed Freon F114 circuit is used for the tests including :

- test compressor,
- water-cooled heat exchanger,
- calibrated nozzle for mass flow measurement,
- throttling valve to regulate the back-pressure,
- electric drive mechanism.

The thermodynamics of Freon F114 are temperature and pressure-dependent and these variations of the thermodynamic parameters have been taken into account. On the other hand, the low speed of sound in Freon 114 makes it more convenient than air for low speed rotors with a comparable Reynolds number range.

Experimental techniques

Measurements upstream of the impeller give the main characteristics of the inlet flow. Downstream of the impeller and in the diffuser, measurements are taken at three different test sections (Fig. 3) :

- the throat of the vaned diffuser (test section n° 1),
- the channel outlet of the vaned diffuser (test section n° 2), in a section orthogonal to the mean streamline and containing a diffuser blade trailing edge,
- the exit radius of the vaned diffuser (test section n° 3).

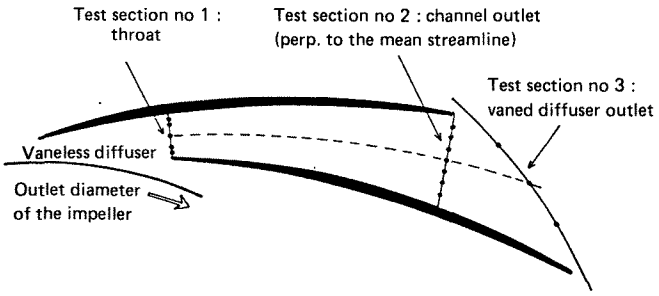

Fig. 3 — Location of measurement stations in the vaned diffuser.

Several taps give the static pressure on both walls at each of these test sections. A great many taps also give the static pressure in the vaneless diffuser, in the semi-vaneless diffuser and between the throat and the channel outlet of the vaned diffuser.

Each of the three test sections is instrumented with probe carrier attachments for pressure probes or single hot wire anemometers to make transverse measurements between the two walls.

In test section n° 1 (throat of the vaned diffuser), a very thin pressure probe give the local time-averaged total pressure. So as not to disturb the flow field, the diameter of this probe is 0.6 mm. Due to the length of the head probe, it cannot measure the local time-averaged flow angle. This angle is calculated from the mean voltage output by the calibrated single hot wire anemometer during the unsteady measurements. In the throat, time-dependent measurements of the flow Mach numbers and flow angles are also measured by means of the single hot wire anemometer, 1.5 mm long and 5 μm in diameter.

In test sections n° 2 and 3, a calibrated pressure probe with two lateral pressure holes measures the local time-dependent flow total pressure and time-dependent flow angle.

However, no measurements can be taken of the velocity component normal to the diffuser walls. This component plays a role in secondary flow regions.

These probes are fit on a probe carrier attachment in order to make measurements at several crosswise stations between the two walls.

There are two drawbacks to using small-diameter hot wire anemometers in transonic air compressors :

- the passband range is too small,
- the wires themselves are not strong enough to resist the aerodynamic forces.

Furthermore, most transonic compressors operate in open circuits and the dust deposit on the wires quickly deteriorates the probe.

Using Freon as a working fluid in a closed loop compressor facility remedies these problems since transonic flows are obtained at low flow velocity and low temperature rises with low speed of impeller rotation.

The two pressure probes have been calibrated along with the hot wire anemometer in a freon loop transonic wind tunnel.

The mean values of the flow characteristics in the diffuser outlet are computed from the measured mass flow, flow temperature and several static pressures measured on both walls at the impeller outlet.

It was assumed that the process in the diffuser was adiabatic and that the flow field is homogeneous without blockage factor. The main flow characteristics at the impeller outlet are indicated in Table III for the design flow rate and rotor speed.

Static pressure ratio	1.919
Total pressure ratio	3.128
Absolute Mach number	0.962
Absolute flow angle from tangential direction	15.35°

Table III : Main flow characteristics at the impeller outlet

Time-averaged measurements in the vaned diffuser throat

The time-averaged total pressure and flow angle are measured at five locations and at twelve depths.

With the mean static pressure picked up at five locations on both walls, these measurements give the contour map of the time-averaged Mach number (Fig. 4). Except the boundary layer effects, more flow discharges in the vicinity of the front wall.

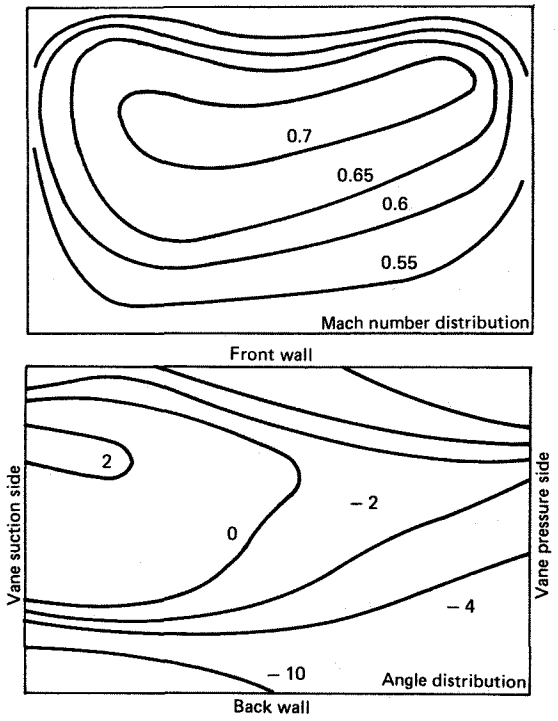

Fig. 4 — Time-averaged flow measured at the vaned diffuser throat.

This fact was observed in measurements made near the impeller equipped with a large vaneless diffuser [3]. We conclude that the axial flow heterogeneities do not change greatly in the semi vaneless diffuser area.

Figure 4 also shows the contour maps of the time-averaged flow angles. Zero degree corresponds to the direction orthogonal to the throat. The ideal flow angle distribution, according to the local vane geometry would be four degrees along thevane suction side, minus four degree along the vane pressure side and zero degree in the middle of the throat.

In fact, experimental results disagree. Near the suction side, the streamline angles are always smaller than four degrees. Very small flow angles are found in the two corners of the throat located along the vane pressure side.

In the vicinity of the both sidewalls, local time-averaged angles are very small.

This is due to the distortion effect of the three-dimensional boundary layer in the vaneless and semi-vaneless diffuser with a strong positive pressure gradient.

In the blade-to-blade direction, Mach number heterogeneities are also large and less flow discharges in the corner consisting of the back wall and the blade pressure side.

Time-dependent measurements in the diffuser throat

The period T corresponds to the passage of two impeller long blades in front of one diffuser vane leading edge. To a definite time t corresponds a dedimensionalized t/T giving the location of the impeller long blades.

The high-frequency measuring system used produces 240 data acquisitions during the period T. From this volume of data, we can plot 240 maps of the instantaneous flow angle and Mach number, giving a precise and continuous time evolution of the flow field structure. Eight of these location impellers have been selected to illustrate the unsteady flow phenomena within the diffuser throat (Fig. 5).

The small drawings show the impeller blade position in sequence and indicate the corresponding dedimensionalized period t/T. The contour maps, to the left of these drawings, illustrate the instantaneous flow angles. The instantaneous Mach number distributions are plotted on the right.

A local flow perturbation generated by the impeller moves through the throat area from the vane pressure side to suction side. This is due to the delay of the fluid, whose streamlines are located in the vicinity of the vane suction side.

During the period T, the instantaneous flow angles never correspond to the ideal angle distribution computed from the vane angles. Flow angles are mainly directed towards the vane pressure side. Furthermore, near the vane suction wall, the flow angle never corresponds to the vane angle in spite of the vane's guidance. It seems that the fluid does not adhere to the wall.

Unsteady separation and axial velocity component are then expected.

In the vicinity of the vane pressure side (leading edge) considerable flow angle variations are observed due to the proximity of the impeller outlet and the lack of guidance of the vane wall.

The wake and jet flow from the impeller blades can be observed easely. For example, considerable Mach number amplitude variations occur in the throat corner consisting of the front wall and the vane pressure side.

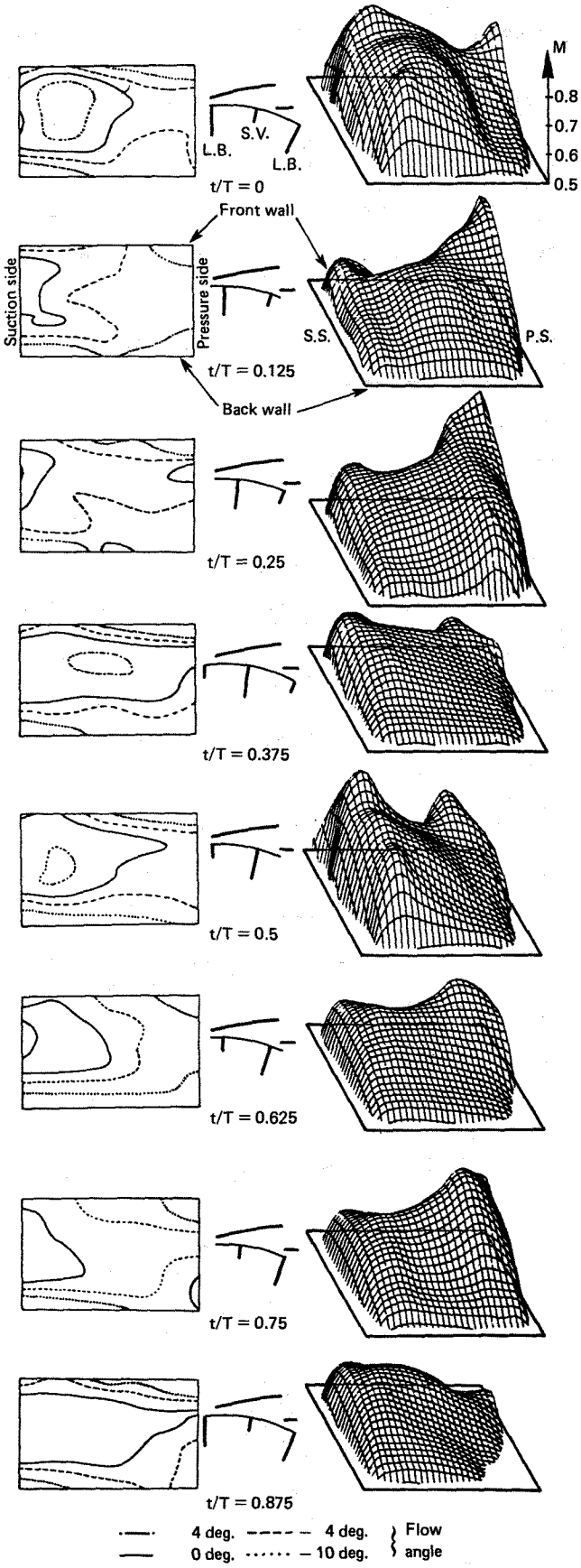

Fig. 5 – Distributions of the Mach number and angle in the throat versus the blade impeller locations.

The variations of the instantaneous flow structure during the first half-period do not correspond to the variations during the second. This is due to the different flow pattern discharged from two impeller channels separated by a splitter vane.

In the middle of the throat, the unsteady flow patterns delivered from the impeller remain large in amplitude [4]. The flow angle fluctuations are about eight degrees and the flow Mach number fluctuations are 12 %. Almost the same values were obtained at an identical radius, when the compressor was equipped with a large vaneless diffuser [3].

Meanwile, the unsteady boundary layer effects contribute to the decreasing amplitude of flow fluctuations and the fluid approaches steady state conditions near the walls.

Measurements at the diffuser divergent channel outlet

The contour maps of the time-averaged Mach number and flow angle are shown Fig. 6.

The flow heterogeneities are higher than in the throat. Outside of the boundary layer, the Mach number distribution across the pitch has a strong maximum in the vicinity of the vane suction side. As in the throat, the flow remains near the front wall. In this area, the flow angle corresponds to the vane angle.

Along the front wall, the large flow angle reveals a three-dimensional boundary layer.

The sharp drop in the Mach number in the vicinity of the pressure side is remarkable. Local flow angles became smaller than the vane angle. In this area, secondary flow and separation are expected. These are certainly due to the flow heterogeneities and three-dimensional boundary layer observed in the throat.

The probe cannot provide the axial components of the streamline. However, these are certainly important in this test section.

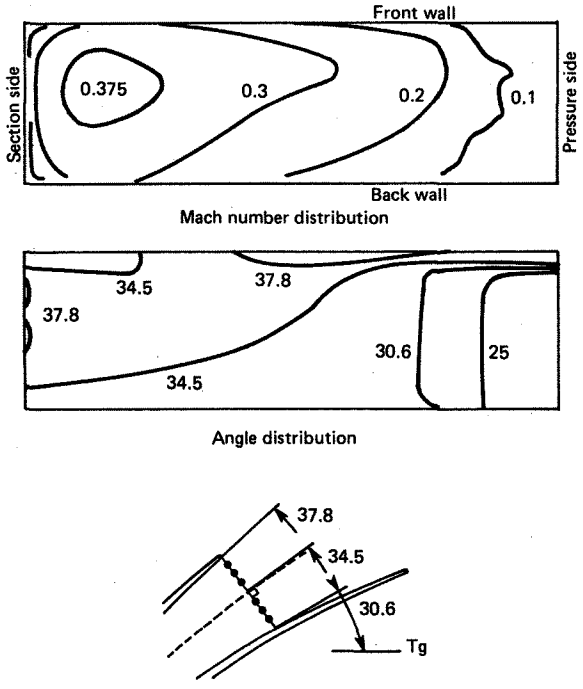

Fig. 6 – Time-averaged flow measured at the vaned diffuser outlet (section 2).

Measurements at the diffuser outlet

Measurements made at the three locations in the vaned diffuser outlet confirm the large and increasing heterogeneities of the flow structure. Figure 7 shows the Mach number and angle versus the dedimensionalized depth ξ of the channel. We find an enlargement of the secondary flow area because the flow Mach number becomes smaller and smaller in the vicinity of the pressure side [5]. This is due to the greater increase of the static pressure in the pressure side streamlines than in the section side streamlines.

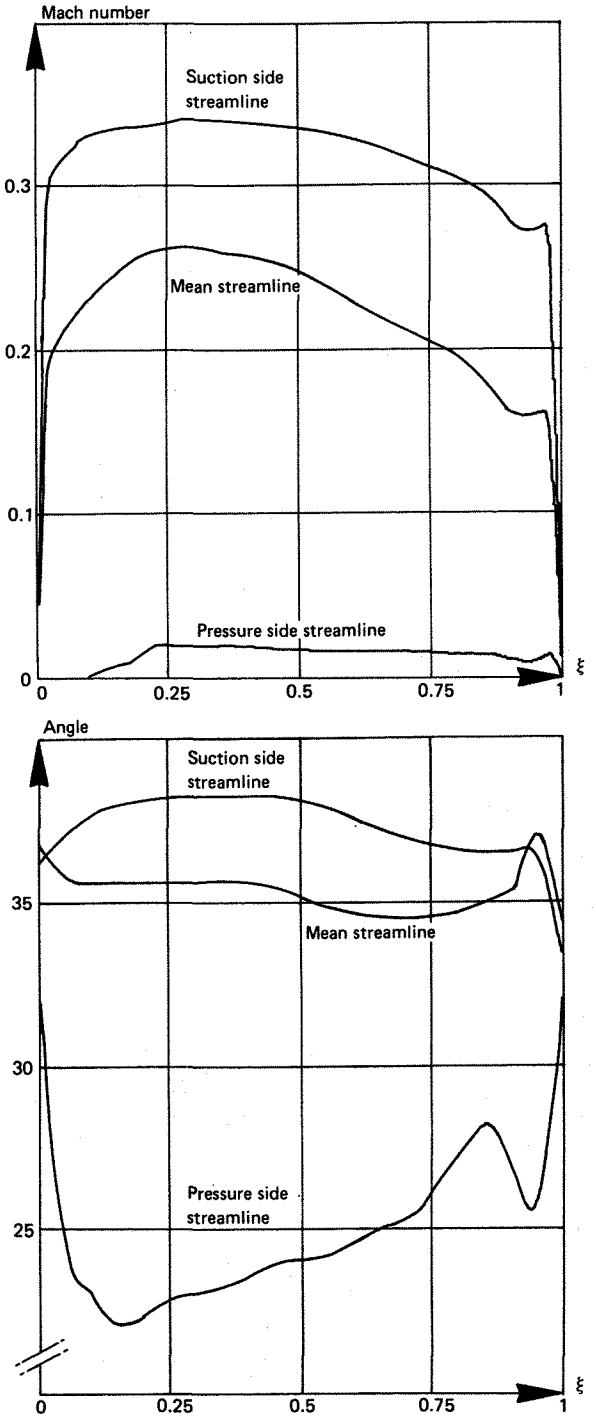

Fig. 7 – Time-averaged flow measured at the vaned diffuser outlet (section 3).

In fact, the flow field structure at the vaned diffuser outlet can be described schematically as a jet-wake configuration with accumulation of loss in the vicinity of the pressure surface.

This impairs the efficiency of the vaned diffuser and does not give an ideal inlet flow to the next compressor stage. Unsteady flow angle measurements were made in the middle of the channel. Flow angle damping is observed as its amplitude decreases to about 2.5 degrees.

Computation of the mean flow field

To determine the performance of each part of the diffuser and to understand the behaviour of the flow field heterogeneities better, it would be desirable to represent correctly the real flow by uniform steady flow models [6]. Many different averaging procedures have been proposed in the literature. However, these mean values are not consitent with all conservation laws. In fact, the specification of an averaging method depends essentially on the intended application.

In order to estimate the heterogeneity level of the flow field at the impeller outlet and its evolution in a vaned diffuser, we can introduce a channel blockage factor B. Using a conventional jet-wake representation, we can assume that the flow vanishes in a fraction B of the test section and the homogeneous equivalent flow discharges in the remaining (1-B) fraction. Using the conservation law for entropy and assuming that the flow temperature measured at the compressor outlet corresponds to the mean temperature flow $\overline{T}_i$, the following equations give the mean total pressure ratio

$$\overline{S}_i = \frac{\int_A S_i \, dQ}{\int_A dQ}$$

$$\overline{\pi}_i = \frac{\overline{P}_i}{P_1} = \left(\frac{\overline{T}_i}{T_1}\right)^{\frac{\gamma}{\gamma-1}} \cdot e^{-\left(\frac{S_i - S_1}{r}\right)}$$

However, the mean static pressure calculated with the momentum law differs from the pressure actually measured. This is a drawback if one wants to calculate the mean absolute Mach number and determine the performance of the diffuser.

To overcome this problem, we use the mean static pressure ratio $\overline{\pi}$ measured from static pressure taps located on both walls of the tested section

$$\overline{\pi} = \frac{\int_A \pi \, dQ}{\int_A dQ}$$

The mean flow angle $\overline{\alpha}$ with regard to the tested section is given from the momentum law on the plane parallel to the section

$$\overline{M} \sin \overline{\alpha} = \frac{1}{Q} \int_A M \sin \alpha \, dQ$$

The blockage factor B is determined according to the following equation

$$B = 1 - \frac{Q}{A \, \overline{\rho} \, \overline{a} \, \overline{M} \cos \overline{\alpha}}$$

Table IV shows the main results. These show the decrease of the mean total pressure ratio $\overline{\pi}_i$ and the blockage factor B along the vaned diffuser.

With these data, total pressure ratio at the impeller outlet was calculated from the local static pressure, the mass flow, Euler's theorem and assuming that there is no blockage factor (B = 0).

In the diffuser outlet section, assuming no losses from the outlet channel, we can compute the local blockage factor.

The blockage factor increases continuously throughout the vaned diffuser.

Test section	$\overline{\pi}_i$	$\overline{M}$	B
2 (Impeller outlet)	3.128	0.962	0 (hyp)
3 (throat)	2.985	0.622	0.047
4 (diffuser channel outlet)	2.933	0.300	0.231
5 (diffuser outlet)	2.933 (hyp)	0.289	0.285

Table IV : Mean characteristic of the flow in each section tested

Performance of the vaned diffuser

The performance of the vaned diffuser between the sections ① and ② can be characterized by the total pressure loss coefficient K

$$K = \frac{\overline{P}_{i\,①} - \overline{P}_{i\,②}}{\overline{P}_{i\,①} - \overline{P}_{①}}$$

and the local real static pressure recovery

$$C_{P_{real}} = \frac{\overline{P}_② - \overline{P}_①}{\overline{P}_{i\,①} - \overline{P}_①}$$

From the computed ideal static pressure recovery we find the efficiency of each part of the vaned diffuser

$$\eta = \frac{C_{P\,real}}{C_{P\,ideal}}$$

Table V indicates the performances of differents zones of the vaned diffuser. Results are comparable to those given by several authors [7] [8]. Due to the highly distorted flow delivered by the impeller and the strong adverse pressure gradient, losses are greater in the semi-vaneless diffuser than in the diffuser channel.

Inlet section	Outlet section	K	$C_{p\ real}$	η
(Impeller outlet)	Vaned diffuser throat	0.118	0.420	0.671
(Impeller outlet)	Channel diffuser outlet	0.161	0.725	0.774
(Impeller outlet)	Diffuser outlet	-	0.732	0.775
Vaned diffuser throat	Channel diffuser outlet	0.093	0.659	0.859

Table V: Performance of each part of the vaned diffuser

Conclusions

A detailed experimental analysis has been made of the flow field in the throat and in the outlet of a diffuser channel.

The transonic centrifugal impeller used has backward leaning blades and is equipped with splitter vanes. The vaned diffuser is of the cambered vane type.

The following conclusions were drawn from the investigations.

1) The distribution of the time-averaged flow Mach number and flow angle is very heterogeneous in both the axial and tangential directions. Due to the strong adverse pressure gradient in the semi-vaneless diffuser, three-dimensional boundary layers are observed near the front wall and back wall.

2) Time-dependent measurements reveal that the flow structure is highly unsteady in the diffuser throat. The blade-to-blade heterogeneities delivered by the impeller do not decrease rapidly in the semi vaned diffuser.

3) Time-averaged measurements performed at the vaned diffuser outlet show that the flow distortions increase in the divergent channel. More massflow is located near the vane suction side. Secondary flow is found in the vicinity of the vane pressure side. Separation occurs at the diffuser outlet.

4) Mean flow characteristics are calculated in the tested sections. The performance of each part of the vaned diffuser has been estimated.

References

[1] D. ECKARDT "Instantaneous Measurements in the Jet-Wake Discharge Flow of a Centrifugal Compressor Impeller". ASME Paper N° 74-GT-90, 1974.

[2] BAMMERT-RAUTENBERG "On the Energy Transfer in Centrifugal Compressors". ASME Paper N° 74-GT-121, 1974.

[3] Ch. FRADIN "Investigation of the Three-Dimensional Flow near the Exit of Two Backswept Transonic Centrifugal Impellers". ISABE, Cincinnati (USA), 1987.

[4] H. KRAIN "A Study on Centrifugal Impeller and Diffuser Flow". ASME Paper N° 81-GT-9, 1981.

[5] D.P. KENNY " A Novel Low-Cost Diffuser for High-Performance Centrifugal Compressors". Journal of Engineering for Power. Jan. 1969.

[6] M. PIANKO "Ecoulements Moyens dans une Turbomachine". In AGARD Proceedings of WG14, 1980.

[7] G. VERDONK "Vaned Diffuser Inlet Flow Conditions for a High Pressure Ratio Centrifugal Compressor". ASME Paper N° 78-GT-50, 1978.

[8] W. STEIN - M. RAUTENBERG "Analysis of Measurements in Vaned Diffusers of Centrifugal Compressors". ASME Paper N° 87-GT-170.